

Optimized Design of the Insulating Gas Layer in Solar Thermal Collectors

Pascal Leibbrandt, Thomas Schabbach

Institut für Regenerative Energietechnik, University of Applied Sciences Nordhausen (Germany)

Summary

The aim of the investigations shown here is to further investigate the convective heat losses in insulation gas layers. These investigations are relevant for the design of the thickness of the insulation gas layer, as this is a main factor influencing the reduction of convective losses. The example used here of the solar glass collector is an extension of the insulating glass collector. The studies on the solar glass collector led to the results shown here, too. In recent studies based on CFD simulations and experimental measurements, deviations from the standard calculation approach by Hollands (1976) are identified and corrected with a correction function. The results shown here apply this correction function to the dimensioning of the thickness of the insulation gas layer. The convective heat transfer coefficient in the gas layer differs up to approx. 30% regarding Hollands (1976).

Keywords: Heat Transfer, Convective Heat Transfer, Conductive / Quasi-Conductive Regime, Calculation Approach, Insulating Glass, Solar Collector, Glass Cavity, Correction Function

1. Problem Definition

To guarantee an optimal collector efficiency, the convective front loss through the insulating gas layer is investigated. The gas volume, filled with insulating gas or air has a length L_{20} , a width B_{20} and a thickness s_{20} , see fig. 1. The resulting aspect ratio is $AR = AR_{20} = L_{20}/s_{20}$.

The most used approach to calculate the convective heat transfer was investigated by Hollands (1976) using an aspect ratio of $AR = 48$. The boundary conditions / assumptions are also: isothermal glass surface temperatures $T_{11}(x, y)$ and $T_{33}(x, y)$, respectively T_{13} and T_{31} , a gas layer pressure p_{20} and a tilt angle φ .

Other research also dealt with experimental and theoretical approaches to the determination of the convective heat transfer coefficient in gas layers. Especially Bartelsen (1993) and Föste (2013) showed that measured data from flat-plate collectors led to higher heat transfer coefficients about 10% regarding to Hollands (1976). Measurements by Föste (2013) on insulating glass collector showed a deviation up to 32%. Yiqin (1991) also investigated mean differences up to 10% in the heat transfer. Eismann (2015) presents analytically derived correction parameter, which was adapted to non-isothermal boundary conditions and highly selective coatings. Own results of the authors Leibbrandt (2016), Leibbrandt (2017) and Leibbrandt (2018) describe recent CFD simulations that deal with the topic and reveal new findings. The aim of the investigations presented here is to determine the convective heat transfer coefficient $h_{20,c}$ in the gas layer between the surfaces (13) and (31), see fig. 1.

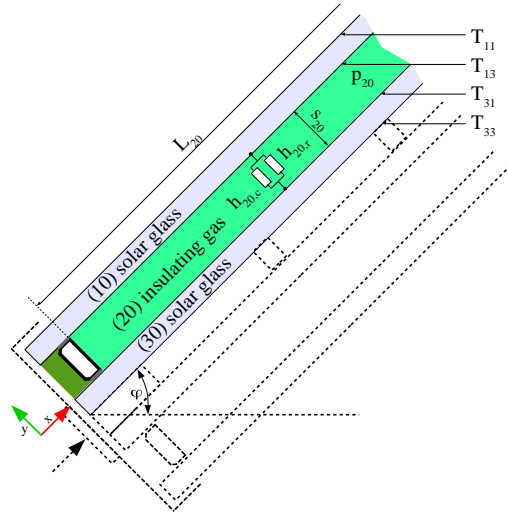


Fig. 1: Geometry and boundary conditions

2. Heat transfer in enclosed Insulating Gas Layers heated from below

The heat losses at the front of the collector are largely determined by internal free convection and radiation. The heat transfer flow is

$$\dot{Q} = A_{20} \cdot h_{20} \cdot (T_{31} - T_{13}) \quad (\text{eq. 1})$$

With the area $A_{20} = L_{20} \cdot B_{20}$. The total heat transfer coefficient h_{20} consists of the shares for the convective heat transfer coefficient $h_{20,c}$ and the radiative heat transfer coefficient $h_{20,r}$. It is

$$h_{20} = h_{20,c} + h_{20,r} \quad (\text{eq. 2})$$

The convective heat transfer coefficient $h_{20,c}$ is calculated from the Nusselt number Nu , which is specified for free convection from eq. 3 with the Rayleigh number Ra ,

$$Nu = Nu(Ra) \quad (\text{eq. 3})$$

Hollands (1976) developed the following eq. from experimental measurements. The eq. is split in three parts, depending on the Rayleigh number considered in the problem. The part [...] + activates the terms in brackets for different Rayleigh numbers regimes. It is [...] + = (|[...]| + [...])/2.

$$Nu = 1 + 1.44 \cdot A \cdot [B]^+ + [C]^+ \quad (\text{eq. 4})$$

With:

$$A = 1 - \frac{1708 \cdot (\sin(1.8 \cdot \varphi))^{\frac{1}{6}}}{Ra \cdot \cos(\varphi)} \quad B = 1 - \frac{1708}{Ra \cdot \cos(\varphi)} \quad C = \left(\frac{Ra \cdot \cos(\varphi)}{5830} \right)^{\frac{1}{3}} - 1 \quad (\text{eq. 5})$$

With the factors B and C the modified Rayleigh number $Ra^* = Ra \cdot \cos(\varphi)$. This is necessary because the flow must be characterized into three flow regimes:

- At lower Rayleigh numbers ($Ra^* < 1708$) the conductive behavior dominates, since the flow velocities are very small. This flow regime is called quasi-conductive regime.
- With increasing Rayleigh numbers ($1708 < Ra^* < 5830$) the flow velocity increases and a monocellular basic flow develops: The gas particles rise at the hot underside, are deflected in the head area of the gas volume and sink again at the cold upper side. In this range of Rayleigh numbers the regime is called monocellular flow or post-conductive.

- With an even higher Rayleigh number ($Ra^* > 5830$) the monocellular flow decays into a multicellular flow with several convection rolls. Flow reversals now also takes place within the gas volume. This flow type is called multicellular flow regime.

To ensure a low heat transfer coefficient in the gas layer and thus a good collector efficiency due to low heat losses, the distance s_{20} should be designed in the way that $Ra^* = 1708$ where the insulating effect of the gas is at its maximum, the convective behavior and thus the heat transfer coefficient are minimum.

In eq. 4 and 5, this point is equal to $B = C = 0$ and $Ra^* = 1708$. For that state with $Ra^* < 1708$ and $Nu = 1$ all present approaches including Hollands (1976) use $Nu = 1$ just from theory without any measurements.

For the conductive regime ($Ra^* < 1708$), Hollands (1976) assumes $Nu = 1$, which corresponds to the case of pure heat conduction. However, pure heat conduction would only occur if the heat flow field is one-dimensional and a stagnant fluid is assumed. But as soon as the heat flow field deviates from the ideal one-dimensional case or as soon as also flow velocities occur in the gas layer $Nu > 1$ should be assumed.

Based on previous CFD simulations further influencing parameters are identified for determining the convective heat transfer coefficient in the gas layer. The experimental setup according Hollands (1976) was simulated in a 3D CFD simulation to validate the used physical models and the discretization. Simplified preliminary CFD investigations are carried out to analyze the flow phenomena in the gas layer. Thus, it is possible to investigate the variety of parameters such as boundary conditions and geometric parameters. With the CFD simulations, it is shown that the heat transfer coefficient depends on the geometry and boundary conditions. This results for different AR in a variation of the Nusselt number. Beside the results for $Ra^* > 1708$, the CFD simulations also show a dependency $Nu(AR)$ for $Ra^* < 1708$. Also the assumption that $Nu > 1$ could be proven for $Ra^* < 1708$ with this CFD simulations.

3. Experimental Investigations

For experimental investigation, insulating glazings with the following design are measured in a test facility according to DIN 12664 (2001). The three insulating glazings examined have the basic dimensions of 500 x 500 mm. The construction of the insulating glazings consists of a 4 mm single-pane safety glass (ESG) pane, the insulating gas layer (here argon) between the panes and a further 4 mm ESG pane. The edge seal consists of an aluminium spacer with butyl as the primary seal and a secondary seal made of thiokol. Under consideration of the size of the spacer (10 mm) the resulting length of the gas layer is 480 mm. The layer thicknesses in the experiment (10.0, 8.0, 6.0 mm) can be adjusted by different thicknesses of the spacer. The resulting aspect ratios AR are 48.0, 60.0 and 80.0.

In the test facility for thermal conductivity measurements according to DIN 12664 (2001) a one-dimensional constant and uniform heat flow density is generated for plane shaped homogeneous sample bodies (here insulating glazings) with plane, plane-parallel surfaces. The test device therefore consists of a central measuring section (evaluation area) in which the measurement is carried out and a surrounding protection ring (guarded hot plate setup). After setting a stationary state in the measurement section, the heat flow density is calculated from the measurement of the heat flow and the evaluation area through which the heat flow passes. The temperature difference between the surfaces of the insulating glass is measured with temperature sensors on the surface of the insulating glass.

As boundary conditions for the experiment, the insulating glass mean temperatures is 20.0, 40.0, 60.0, and 80.0 °C at temperature difference of 20 K for each set. The measurement is carried out for tilt angles of 0, 20, 40 and 60°.

The convective heat transfer coefficient $h_{20,c}$ is calculated with the overall thermal resistance of the insulating glass and under consideration of the thermal resistances of the glass panes and the radiative heat transfer coefficient $h_{20,r}$. The resulting deviations between $h_{20,c}$ and the heat transfer coefficient according to Hollands (1976) h_{Holl} lead to the following correction function regarding Nu (for $48 \leq AR \leq 80$ and $Ra^* < 1708$).

$$D = D_2 \cdot AR^2 + D_1 \cdot AR + D_0 \quad (\text{eq. 6})$$

With: $D_2 = 1.292 \cdot 10^{-4}$, $D_1 = -2.283 \cdot 10^{-2}$ and $D_0 = 2.035$

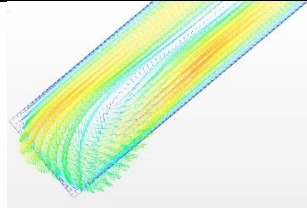
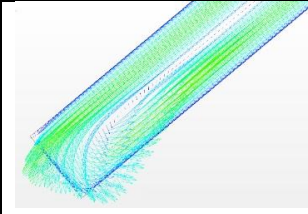
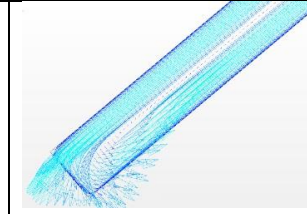
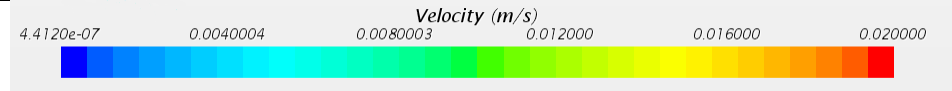
This leads to the proposal of a corrective term \mathbf{D} for eq. 7. \mathbf{D} should just be used for $Ra^* < 1708$ and is only experimental proved for $48 < AR < 80$. The resulting adapted equation is now:

$$Nu = 1 + \mathbf{D} + 1.44 \cdot A \cdot [B]^+ + [C]^+ \quad (\text{eq. 7})$$

Simplified 2D simulations with the boundary conditions analogous to the measurements confirm the measurement results and the dependence of the heat transfer coefficient on the aspect ratio. Further deviations can also be determined from the simulations for other aspect ratios. As the aspect ratio increases, the layer becomes specifically thinner and the viscous effects dominate over the buoyancy forces. The ratio between buoyancy and viscosity within the fluid changes. This results in lower flow velocities within the layer, which means that the heat transfer is more influenced by conduction than by convection. The heat transfer coefficient and the corresponding Nusselt number Nu thus increases for lower aspect ratio AR due to higher mean flow velocities u .

$$AR \downarrow \rightarrow u \uparrow \rightarrow Nu \uparrow$$

Tab. 1: Overview simplified 2D simulations

φ	40°	40°	40°
T_{13} / T_{31}	70 / 90 °C	70 / 90 °C	70 / 90 °C
AR	48	60	80
Nu	1.27	1.16	1.04
u_{max}	17.87 mm/s	10.77 mm/s	5.72 mm/s
Velocity Field			
			

4. Results

The propagated correction function and optimized design of the insulating glass layer (here thickness s_{20}) is done here for two operation points. The use of the correction function leads just to a small change in the insulation layer thickness but shows an even higher convective heat transfer coefficient in the range of approx. +30% for small AR and approx. +10% for large AR and $Ra^* < 1708$.

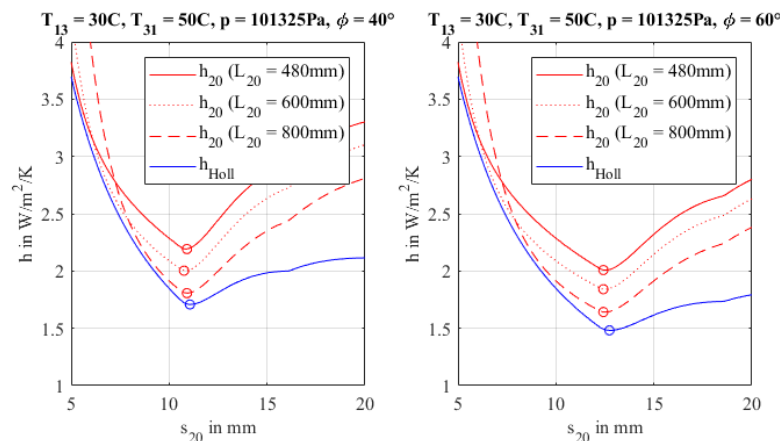


Fig. 2: Heat transfer coefficients in gas layer with correction function

These changes in the investigated field of $Ra^* < 1708$ do not lead to a significant change in the design of flat-plate or insulating glass collectors, but must be taken into account in the collector and system simulation.

5. References

- Bartelsen, Janßen, Rockendorf, 1993. Heat Transfer by Natural Convection in the Air Gap of Flat Plate Collectors. Proceedings ISES Solar World Congress, pp. 267-273, Budapest, Ungarn
- Eismann, 2015. Accurate analytical modeling of at plate solar collectors: Extended correlation for convective heat loss across the air gap between absorber and cover plate. Solar Energy 122, 1214 – 1224
- DIN 12664, 2001. Wärmetechnisches Verhalten von Baustoffen und Bauprodukten. Bestimmung des Wärmedurchlasswiderstandes nach dem Verfahren mit dem Plattengerät und dem Wärmestrommessplatten-Gerät – Trockene und feuchte Produkte mit mittlerem und niedrigem Wärmedurchlasswiderstand. Deutsche Fassung EN 12664:2001. Berlin
- Föste, 2013. Flachkollektor mit selektiv beschichteter Zweischeibenverglasung. Dissertation, Gottfried Wilhelm Leibniz Universität Hannover
- Hollands, Unny, Raithby, Konicek, 1976. Free Convective Heat Transfer Across Inclined Air Layers. J. Heat Transfer 98(2), 189-193
- Leibbrandt, Schabbach, Dölz, Rhein, 2016. CFD-Untersuchungen zu konvektiven Wärmeverlusten in Scheibenzwischenräumen mit großem Seitenverhältnis. 26. OTTI Symposium Thermische Solarenergie, Bad Staffelstein
- Leibbrandt, Schabbach, Dölz, Rhein, 2017. Experimental and CDF Optimization on Flow and Heat Transfer to a Solar Flat-Plate Glass Collector. Solar World Proceedings ISES Solar World Congress, Abu Dhabi
- Leibbrandt, Schabbach, Dölz, Rhein, 2018. Untersuchungsergebnisse zur Strömung und Wärmetübertragung im Nurglaskollektor. 28. OTTI Symposium Thermische Solarenergie, Bad Staffelstein
- Yiqin et al., 1991. Measured Top Heat Loss Coefficients for Flat Plate Collectors with Inner Teflon Covers. Proceedings of the Biennial Congress of the International Solar Energy Society, Denver, Colorado